Available online at www.sciencedirect.com

ScienceDirect

Ceramics International 42 (2016) 1552–1562

CERAMICS INTERNATIONAL

www.elsevier.com/locate/ceramint

Effects of airborne-particle abrasion protocol choice on the surface characteristics of monolithic zirconia materials and the shear bond strength of resin cement

Ji-Eun Moon[a], Sung-Hun Kim[a,*], Jai-Bong Lee[a], Jung-Suk Han[a], In-Sung Yeo[a], Seung-Ryong Ha[b]

[a]Department of Prosthodontics and Dental Research Institute, School of Dentistry, Seoul National University, Seoul, Republic of Korea
[b]Department of Dentistry, Ajou University School of Medicine, Suwon, Republic of Korea

Received 9 September 2015; received in revised form 16 September 2015; accepted 17 September 2015
Available online 25 September 2015

Abstract

This study evaluated the effect of several airborne-particle abrasion protocols on the surface characteristics of monolithic zirconia and of protocol choice on the shear bond strength of resin cement. 375 bar-shaped ($45 \times 4 \times 3$ mm^3) and 500 disk-shaped ($\varnothing 9 \times 1$ mm^2) monolithic zirconia specimens were divided into 25 groups. All specimens were abraded with one of three different sizes of alumina particles (25, 50 or 125 μm), two different pressures (2 or 4 bar), two distinct application times (10 or 20 s) and two distinct incidence angles (45° or 90°). The bar-shaped specimens were used for 3-point bending test; Weibull parameters were calculated and transformed monoclinic phase (X_M), surface characteristics were examined. The disk-shaped specimens were used to determine the shear bond strength of resin cement before and after thermocycling. All data were analyzed using 4-way ANOVA and a multiple comparison Scheffé test ($\alpha = .05$). The particle size, pressure and time significantly affected the flexural strength, while the incidence angle was insignificant. The X_M and surface roughness were proportional to the size, pressure, time and incidence angle. The Raman spectrum analysis showed a higher proportion of the monoclinic phase as the depth of the specimen was closer to the abraded surface. In bonding with resin cement, the highest shear bond strength after thermocycling was obtained by the abrasion with 50 μm particles at 4 bar for 20 s, regardless of incidence angle. Surface treatment of monolithic zirconia with 50 μm particle at 4 bar for 20 s at either 45° or 90° incidence angles is recommended.
© 2015 The Authors. Published by Elsevier Ltd. This is an open access article under the CC BY-NC-ND license (http://creativecommons.org/licenses/by-nc-nd/4.0/).

Keywords: B. Surfaces; C. Strength; D. ZrO_2; E. Biomedical applications; Resin cement

1. Introduction

In response of the high demand for highly esthetic, metal-free and biocompatible restoration materials with high flexural strength, various types of all-ceramic systems have been developed in the last few decades. In a systematic review, all-ceramic crowns showed comparable survival rates to metal–ceramic crowns when used in the anterior and or premolar regions, but had a significantly higher fracture rate when used in the posterior region [1]. Substantial effort has been put forth in the development of more reliable all-ceramic systems. In the early 1990s, yttria-stabilized tetragonal zirconia polycrystal (Y-TZP) was introduced to dentistry as a core material for all-ceramic restorations. Compared to other all-ceramic systems, results with Y-TZP have been encouraging, as it has shown high resistance to fracture [2,3].

Although damage to a zirconia framework has been reported only rarely, chipping or fracturing of the ceramic veneer has been proposed as the most frequent reason for failure of zirconia-based restorations [4–6]. Therefore, in order to increase the success rate of restoration and overcome the chipping problem, zirconia restoration without veneering ceramic, called a monolithic zirconia restoration system, was introduced. Many studies of monolithic zirconia restorations have shown improved

*Corresponding author. Tel.: +82 220722664; fax: +82 220723860.
E-mail addresses: ksh1250@snu.ac.kr (S.-H. Kim), dragon_001@hanmail.net (S.-R. Ha).

http://dx.doi.org/10.1016/j.ceramint.2015.09.104
0272-8842/© 2015 The Authors. Published by Elsevier Ltd. This is an open access article under the CC BY-NC-ND license (http://creativecommons.org/licenses/by-nc-nd/4.0/).

clinical and laboratory results [7–9]. Their strong bond strength is indispensable for the long-term durability of restorations. Manufacturers also claim that zirconia ceramic restorations can be successfully cemented with either conventional or adhesive cements. Nevertheless, some zirconia fixed partial dentures (FPDs) show reduced retention with abutments. A strong, durable resin bond to dental ceramics is established by the formation of chemical bonds and micromechanical interlocking, and achieving reliable and stable bond to zirconia remains a challenge [10,11]. As zirconia has a polycrystalline structure and limited vitreous phase, neither hydrofluoric acid etching nor silanization can achieve durable zirconia-resin bonding [10]. Thus, various surface treatments have been introduced to establish durable adhesion between zirconia and dental resin cement.

For chemical bonding, many studies have shown that functional monomers containing 4-methacryloyloxyethyl trimellitate anhydride (4-META) and 10-methacryloyloxydecyl dihydrogen phosphate (MDP) act as coupling agents [11–13]. Moreover, recent studies showed that zirconia primers and chemically adhesive resin cements have reliable bond strength [13,14].

For mechanical interlocking, airborne-particle abrasion has been used to clean the surface, removes impurities, increases surface roughness, and modify the surface energy and wettability. In addition, airborne-particle abrasion provides the mechanical impingement of particles on the surface [15–17], which results in a roughened surface and allows the resin cement to flow into these micro-retentions and creates a stronger micromechanical interlock [18]. Airborne-particle abrasion with alumina has been identified as a key factor in achieving a durable bond for zirconia-based ceramics [19–21]. Different sizes of abrasive alumina particles have been used, without evidence of the superiority of one over another [10–12,22]. However, recent *in vitro* studies report that airborne-particle abrasion may have a deleterious effect on the zirconia surface due to the creation of microcracks, which might reduce the flexural strength [23,24]. Moreover, the tetragonal phase of Y-TZP is converted to the monoclinic phase with volume expansion (4–5%) under the high stresses caused by airborne-particle abrasion, and this unique transformation can produce different types of damage that affect the structural integrity and material reliability [25,26]. Specifically, this process may result in an increase in the crack propagation resistance of Y-TZP for a certain period of time, functioning as a toughening mechanism [17,27]. Conversely, since the presence of the monoclinic structure is unstable and stressful, there is a higher tendency for the zirconia ceramic in this phase to be fragile. Thus, it may result in an increase in the fracture tendency over the longer term [23,28,29]. The counteracting effects of airborne-particle abrasion on the flexural strength of Y-TZP are controversial in terms of effective power and duration of abrasion, and the role of surface flaws acting as the stress concentrators relative to the stress-induced surface compressive layer [23,30,31].

Although several surface treatments have been recently described [10,18,32–39], the selection of the most appropriate airborne-particle abrasion protocol on for Y-TZP remains controversial. Moreover, no literature describing the phase transformation of monolithic zirconia under various airborne-particle abrasion protocols could be found. Thus, it is necessary to determine the optimum protocol for airborne-particle abrasion for monolithic zirconia restoration, in order to consistently achieve a more favorable clinical outcome.

This study was aimed to evaluate several airborne-particle abrasion protocols and to determine how they affect monolithic zirconia in terms of flexural strength, surface characteristics, and reliability. The shear bond strength between the abraded monolithic zirconia and resin cement was also evaluated. The null hypothesis to be tested was that there was no difference in flexural strength, surface characteristics or shear bond strength of resin cement before and after thermocycling among groups treated with various airborne-particle abrasion protocols.

2. Materials and methods

2.1. Evaluation of microstructural changes in airborne-particle abraded monolithic zirconia ceramic

2.1.1. Preparation of the specimens

Three-hundred seventy-five specimens ($45 \times 4 \times 3$ mm^3) of densely sintered high-purity monolithic zirconia ceramic (Zmatch, Dentaim, Seoul, Korea) – which consisted of 94–95% ZrO_2 and HfO_2, $5 \pm 0.2\%$ Y_2O_3 and $\leq 0.25\%$ Al_2O_3 – were fabricated. The samples, denoted 'as-received', were wet ground in sequence, first with 300 grit diamond grinding disk and sequentially with 6, 3 and 1 μm diamond slurry. The grinding and polishing were performed in order to minimize surface defects on the specimens before testing.

2.1.2. Surface treatment with alumina air abrasion

Bar-shaped specimens were randomized into 25 groups ($n=15$), and for each group a different surface treatment was applied to the top surface of the specimens (Group B to Y). Group A was the control group, with the surface remaining in the 'as-received' state for comparison. For alumina particle abrasion, the specimens were mounted in a sample holder at a distance of 10 mm from tip of the sandblaster unit (AX-B3, AxianMedical Co., Tianjin, China), equipped with a 5 mm diameter nozzle. Specimens were abraded with 25, 50 or 125 μm alumina particles (Cobra, Renfert GmbH, Hilzingen, Germany) at an air pressure of 2 or 4 bar for 10 or 20 s. The incidence angle of particle delivery was maintained at either 45° or 90°. The airborne-particle abrasion protocols for each group are shown in Table 1.

2.1.3. X-ray diffractometry and Raman spectroscopy analyses

Before and after the airborne-particle abrasion, randomly selected specimens from each group were examined to determine the crystalline phases by X-ray diffractometry (D8 DISCOVER, Bruker, Karlsruhe, Germany). X-ray diffraction data was collected using 2θ diffractometer and Cu-Kα radiation. The diffractogram was obtained from 20° to 40° at a scan speed of 5°/min and a step size of 0.02°, covering the location of the highest peaks of *t* and *m* phases. The monoclinic phase peak

Table 1
Experimental groups with the various airborne-particle abrasion conditions.

Group	Size of particle (μm)	Pressure (bar)	Time (s)	Angle (deg)
A (Control)	No treatment			
B	25	2	10	45
C			10	90
D			20	45
E			20	90
F		4	10	45
G			10	90
H			20	45
I			20	90
J	50	2	10	45
K			10	90
L			20	45
M			20	90
N		4	10	45
O			10	90
P			20	45
Q			20	90
R	125	2	10	45
S			10	90
T			20	45
U			20	90
V		4	10	45
W			10	90
X			20	45
Y			20	90

intensity ratio (X_M) was calculated using the method described by Garvie and Nicholson [40].

Raman spectra were collected with a triple monochromator spectrometer (MonoRa 750i, Dongwoo optron, Kwangju, Korea). The Ar laser (488 nm wavelength) beam was focused using an optical microscope with a $\times 100$ long-focal objective. Sample exploration and record spectra were performed in steps of -1 μm.

2.1.4. Scanning Electron Microscopy (SEM), Confocal Laser Scanning Microscopy (CLSM) and Atomic Force Microscopy (AFM) analyses

Randomly selected specimens from all groups were examined using a scanning electron microscope (FE-SEM, S-4700, HITACHI, Tokyo, Japan) at $\times 500$ and $\times 5000$ magnification. Typical cases were used for illustration. Confocal laser scanning microscopy (LSM 5 Pascal, Carl Zeiss Microscopy, Göttingen, Germany) was performed to evaluate the surface roughness (S_a) values of the experimental groups. The measuring area was 450×450 μm^2, and the height of the z-stack was 30 μm in 1 μm intervals.

An atomic force microscope (SPA-400, Seiko instruments, Chiba, Japan), operated in contact mode set to a 10 μm tip height, no rotation of cone angle and 125 μm cantilever length, was used to obtain a quantitative and qualitative data. This created a 3-dimensional image of the microstructural surface, located in the center of the samples.

2.1.5. Flexural strength test

After the different surface treatments, a 3-point bending test was performed at a cross-head speed of 1 mm/min in a universal testing machine (Model 3345, Instron, Canton, MA, USA) according to the ISO 6872:2008 guideline. Maximum load to failure was recorded, and the flexural strength (σ_f) was calculated in MPa.

2.2. Shear bond strength of resin cement

2.2.1. Preparation of the specimens

Five-hundred disk-shaped specimens ($Ø9 \times 1$ mm^2) were fabricated and then sintered in the relevant equipment and randomly distributed into 25 groups ($n=20$). Airborne-particle abrasion protocols were the same as described in Section 2.1.2.

2.2.2. Bonding procedure

All specimens were embedded in polytetrafluoroethylene (PTFE) molds such that the abraded surface of the disk remained uncovered for the application of the resin cement. Commercially available dual-cured resin cement (Panavia F 2.0, Lot no. A paste-00535A and B-paste 00101A, Kuraray Medical Co. Ltd., Osaka, Japan) was chosen because it has the functional monomers (MDP). The resin cement was mixed and packed incrementally into the PTFE ring using a hand instrument and then left to polymerize completely for 30 min at 23 ± 1 °C after a 20 s LED light curing (EliparTM S10, 3M ESPE, St. Paul, MN, USA). After setting, half of the specimens in each group ($n=10$) were subjected to thermocycling for 5000 cycle between 5 and 55 °C. The dwelling time at each temperature was 30 s, and the transfer time from one bath to another was 2 s. The remained subgroups ($n=10$) were tested without thermocycling.

2.2.3. Shear bond strength test

The specimen was mounted in the jig of a universal testing machine (Model 3345, Instron, Canton, MA, USA) and was subjected to the shear stress at a constant crosshead speed of 1 mm/min until a fracture was evident between the zirconia and resin cement. Maximum load to failure was recorded, and shear bond strength was calculated in MPa before and after thermocycling. The fracture surfaces of selected specimens were examined using SEM (FE-SEM, S-4700, HITACHI, Tokyo, Japan) at $\times 30$ and $\times 500$ magnification.

2.3. Statistical analysis

For flexural strength, statistical analyses were performed using 4-way ANOVA and Scheffé multiple comparisons ($\alpha=.05$). The 4 factors used for the analyses were abrasion particle size, pressure, time and incidence angle. In addition to the above measurements, the strength distributions of quasi-brittle materials like ceramics are generally considered to be more properly described by Weibull statistics rather than mean strength values determined using a Gaussian strength distribution [41–43].

In addition, differences in shear bond strength before and after thermocycling were also tested with 4-way ANOVA ($\alpha=.05$). All calculations were performed using SPSS statistical software package (SPSS 20.0; SPSS Inc., Chicago, IL, USA).

Table 2
The influence of alumina particle size, air stream delivery pressure, application time and incidence angle of particle delivery on the flexural strengths, characteristic strengths, Weibull modulus, monoclinic phase contents and surface roughness.

	Control	Experimental																									
Size (μm)	As-received	25								50						125											
Pressure (bar)					4					2			4			2			4							
Time (s)		10		20		10			20			10			20		10			20			10			20	
Angle (°)		45	90	45	90	45	90	45	90	45	90	45	90	45	90	45	90	45	90	45	90	45	90	45	90	45	90
Group	A	B	C	D	E	F	G	H	I	J	K	L	M	N	O	P	Q	R	S	T	U	V	W	X	Y		
Mean strength (MPa)	1454 (93.6)	1245 (72.6)	1179 (74.1)	1498 (207.4)	1597 (165.2)	1725 (218.6)	2047 (274.6)	2695 (283.1)	2554 (215.2)	1697 (179.0)	1682 (165.5)	1580 (173.8)	1679 (234.6)	1568 (209.8)	1320 (191.1)	1356 (219.9)	1346 (177.1)	1330 (137.9)	1351 (115.9)	1410 (138.8)	1541 (119.8)	1412 (150.5)	1426 (152.1)	1618 (179.0)	1525 (226.3)		
σ_0 (MPa)	1496	1279	1212	1597	1668	1823	2176	2827	2656	1778	1758	1660	1794	1671	1413	1457	1426	1393	1404	1478	1596	1483	1494	1734	1628		
m	18	20	18	8	11	9	8	11	14	11	12	10	8	8	8	7	9	11	13	12	15	11	12	11	7		
X_M	0	16	22	25	32	26	31	31	32	27	37	34	36	29	34	34	37	30	33	33	38	35	36	38	40		
S_a (μm)	0.07 (0.002)	0.34 (0.007)	0.34 (0.030)	0.33 (0.015)	0.39 (0.022)	0.49 (0.020)	0.54 (0.013)	0.58 (0.031)	0.64 (0.013)	0.44 (0.032)	0.49 (0.007)	0.50 (0.016)	0.62 (0.018)	0.55 (0.017)	0.58 (0.029)	0.61 (0.010)	0.67 (0.037)	0.44 (0.013)	0.45 (0.019)	0.57 (0.006)	0.58 (0.020)	0.74 (0.013)	0.89 (0.016)	0.84 (0.040)	0.91 (0.055)		

σ_0 = Characteristic strength; m = Weibull modulus; X_M = Monoclinic phase contents; S_a = Surface roughness.

3. Results

The mean flexural strength, characteristic strength (σ_0) and Weibull modulus (m) for the experimental groups are listed in Table 2.

In this study, mean flexural strength ranged from 1179 ± 74.1 MPa to 2695 ± 283.1 MPa, the characteristic strength from 1212 MPa to 2827 MPa, and Weibull modulus from 7 to 20. The specimens tested in the control group showed mean flexural strength of 1454 ± 93.6 MPa, σ_0 of 1496 MPa and m of 18. When specimens were abraded with 25 μm alumina particles, there was a significant increase in the flexural strength compared to that of the control group. However, with the 50 and 125 μm alumina particles, there were no significant differences. Higher pressure and longer abrasion time increased the flexural strength of the 25 μm particle size; abrasion under 4 bar and 20 s resulted in significantly increased strength compared to that at 2 bar and 10 s. However, trends in these tendencies were less unclear with other particle sizes. The 50 μm particle size showed a tendency toward slightly decreased strength with higher pressure and longer time, except for Group M, while the 125 μm particle size showed slightly increased strength with higher pressure and longer time, except for Group Y. Weibull moduli were decreased in experimental groups except for Groups B and C.

According to the 4-way ANOVA for flexural strength measured with the 3-point bending test, we observed that the 3 main factors tested (alumina particle size, pressure and time) all significantly affected the flexural strength; however, the incidence angle did not. Interactions were all significant except for size × incidence angle, pressure × incidence angle, and time × incidence angle. The highest strength specimens resulted from the following parameters: 25 μm particles, 4 bar, 20 s and 45° (Group H, σ_0 = 2827 MPa).

Fig. 1a presents the Raman spectra obtained in Group U at several depths. The tetragonal phase was observed with intense peaks at 147, 265 and 320 cm^{-1}. Conversely, the monoclinic intense peaks at 181 and 190 cm^{-1} were observed in the spectra of the most external area. X_M increased with larger particle size, higher pressure, longer time, and increased incident angle except for Group K, and ranged from 0% (control group) and 16% (Group B) to 40% (Group Y). The X-ray diffraction spectra of the control group and the experimental Group Y, the latter having the highest monoclinic contents among the experimental specimens, are shown in Fig. 1b. The X_M values were 0% and 40%. The group A spectra only have one t peak at 30.2°, while m peaks were shown at both sides of a reduced and broadened t peak in the Group Y spectra. These results confirm that the observed asymmetry in the spectrum of Group Y was due to concentrated the stress in the region of the abraded surface. The relative proportion of the specimens in the monoclinic phases (X_M) is summarized in Table 2.

The surface roughness values (S_a) measured by CLSM are presented in Table 2. The representative surface images showing differences between the groups are shown using reconstructed 3D images of Groups A, B and Y in Fig. 2a–c. The mean surface roughness of specimen ranged from 0.33 ± 0.015 μm to 0.91 ± 0.055 μm. The control group (Fig.

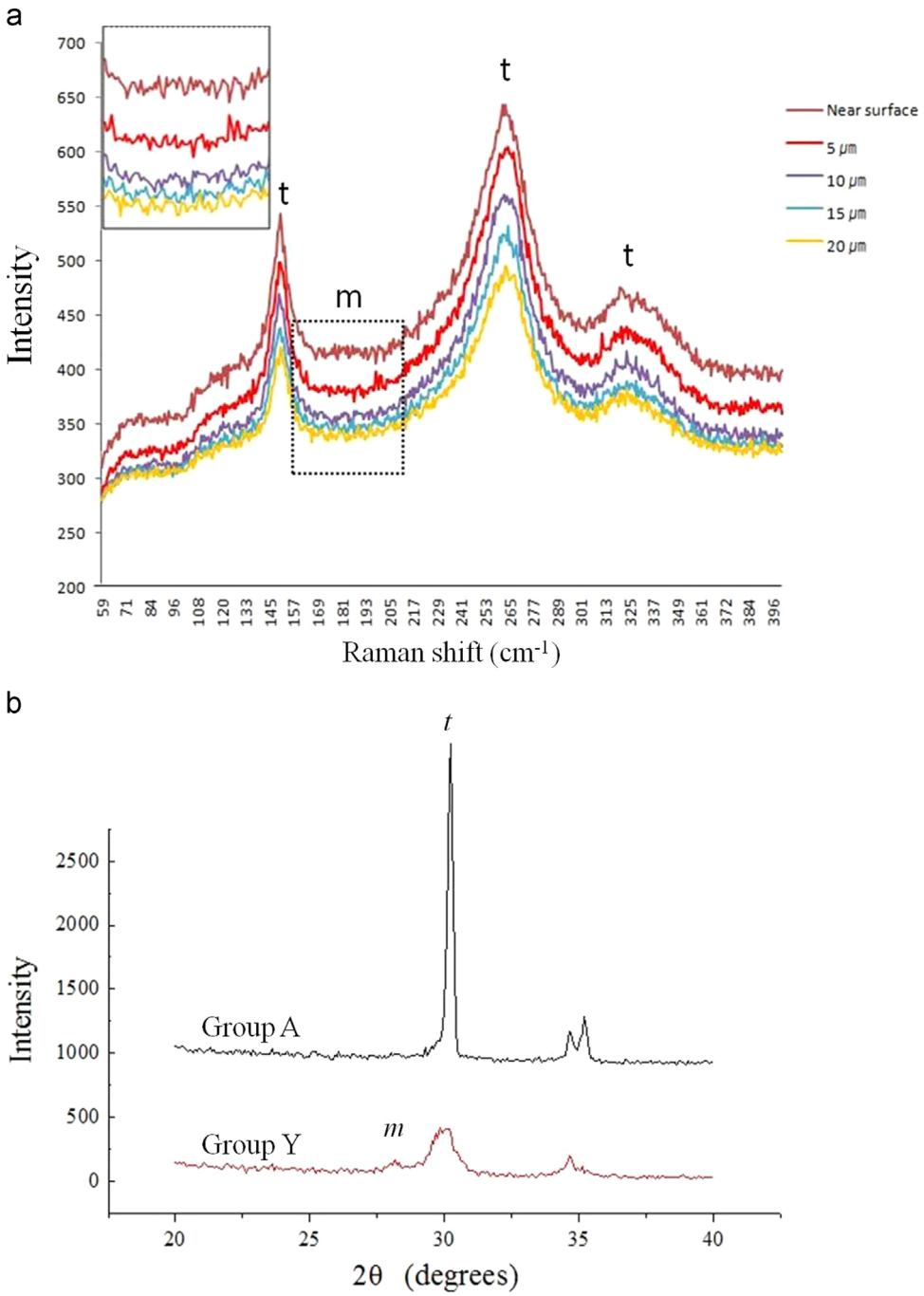

Fig. 1. (a) Raman spectra obtained in Group U at several depths. The monoclinic doublet at 181–190 cm^{-1} is evident in the spectra of the most external area, but closer to surface; (b) X-ray diffraction patterns obtained from Groups A and Y. Graph of Group Y shows the *m* intensity peak near 29° and 31° and shorter *t* peak compared with Group A.

3a) had a mean S_a of 0.07 ± 0.002 μm. Of the test specimens, Group B had the smallest value of 0.34 ± 0.007 μm (Fig. 2b), and Group Y had the highest value of 0.91 ± 0.055 μm (Fig. 2c). The mean S_a increased with larger particle size, higher pressure, longer time and larger incidence angle, except for Groups B and C (Both $S_a = 0.34$ μm).

Microscopic examination revealed changes in the topographic surfaces of monolithic zirconia ceramics after airborne-particle abrasion with alumina (Fig. 3). SEM observations revealed an increase of surface roughness in accordance with the increase of S_a value. In the control group, no micro-retentive pattern could be detected (Fig. 3a and b). After airborne-particle abrasion with 25 μm, the smooth surface was roughened and the polished pattern was no longer seen (Fig. 3c and d). This treatment produced a coarse surface with grooves and sharp edges. With the larger particle size of 125 μm, strong abraded conditions created a similar but more roughened surface (Fig. 3e and f).

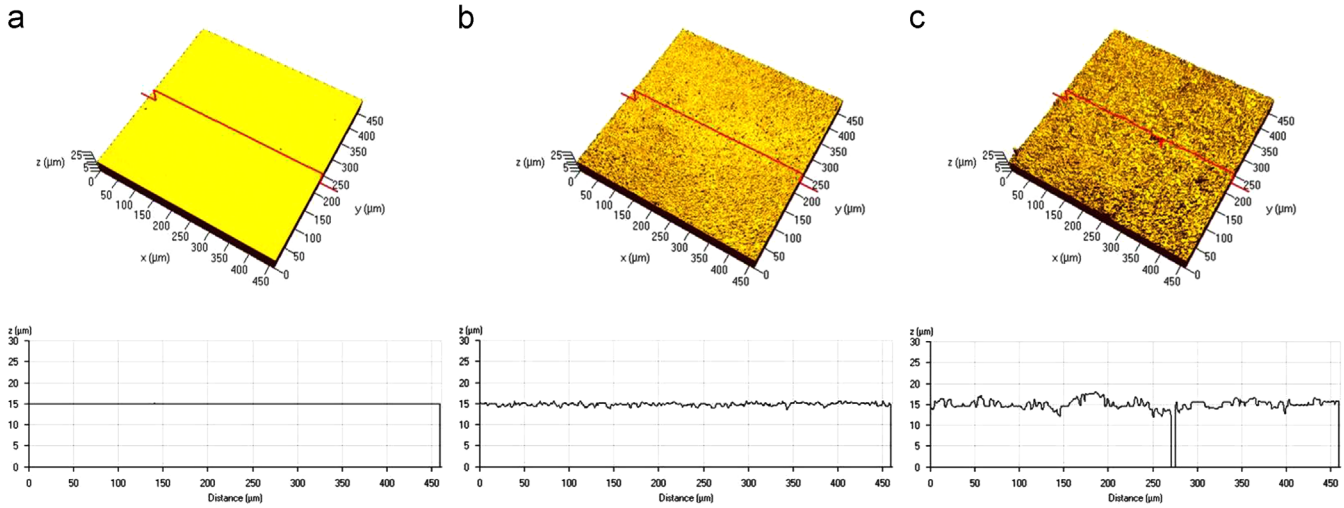

Fig. 2. The representative confocal laser scanning microscopy images of the selected groups: (a) Control group; (b) the smallest S_a value among abraded groups – Group B; (c) the highest S_a value among abraded groups – Group Y.

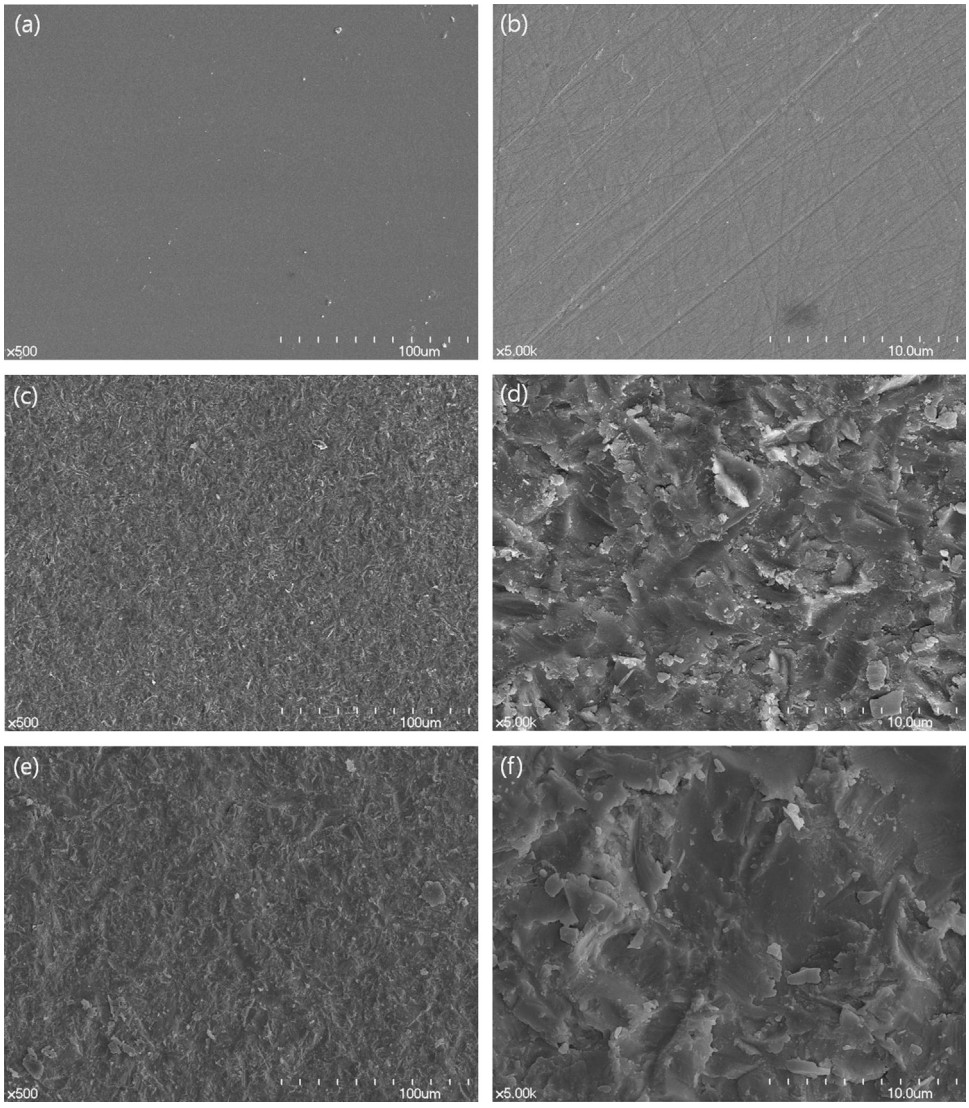

Fig. 3. Scanning electron micrographs (the left sides magnification × 500 and the right sides × 5000) of zirconia surfaces: (a, b) Control group; (c, d) Group B which had the smallest mean S_a value; (e, f) Group Y which had the highest mean S_a value.

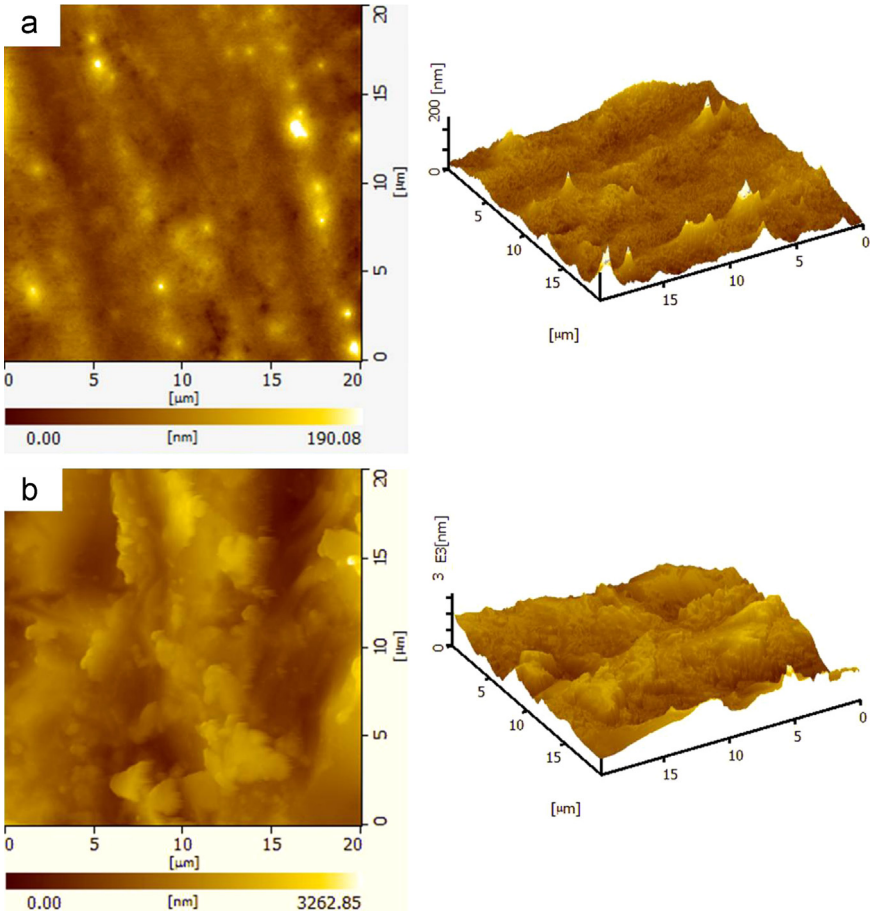

Fig. 4. Representative microstructural images by atomic force microscopy: (a) Control group; (b) Group Y. Control group has the maximum height of 190.08 nm, but Group Y has the maximum height of 3,262.85 nm.

The representative AFM images are shown in Fig. 4. The 'as-received' surface of the control group exhibited a few small spikes and is shown in Fig. 4a. Fig. 4b shows the engraved surface after abrasion with 125 μm, 4 bar, 20 s and 90° (Group Y).

The mean and standard deviations of shear bond strength in all groups are listed in Table 3. In this study, the mean shear bond strength of resin cement ranged from 10.8 ± 2.52 MPa to 18.3 ± 3.64 MPa before thermocycling and from 6.1 ± 2.84 MPa to 12.7 ± 3.38 MPa after thermocycling. The control group showed mean shear bond strength of 6.7 ± 1.92 MPa before thermocycling and 3.0 ± 1.12 MPa after thermocycling. Airborne-particle abrasion significantly increased the bond strength, while thermocycling decreased the bond strength of resin cement. In the thermocycling groups, strong shear bond strengths were observed in specimens abraded with 50 μm, 4 bar, 20 s at both 45° and 90° (Groups P and Q). On the other hand, weak shear bond strengths were observed in specimens abraded with 125 μm, 2 bar and 10 s at both angles (Groups R and S). Specimens abraded with 50 μm particles exhibited significantly higher values on a similar surface roughness level compared with 25 or 125 μm. The 3 main factors (alumina particle size, pressure and time) significantly affected the bonding with resin cement; however, the incidence angle did not. Interaction of alumina particle size × pressure significantly affected the shear bond strength before thermocycling. However, only the interaction of particle size × pressure × time was statistically significant after thermocycling. This means that the effects of each of the factors individually did not account for the results observed with the combination of particle size × pressure × time that resulted in higher shear bond strength after treatment with the aging process. The group with the highest bond strength was obtained with 50 μm particles at 4 bar for 20 s, using either 45° or 90°.

Fig. 5 shows the representative SEM images of the fractured interfaces in control group, Group R and Group Q, each having shear bond strength of 3.0 ± 1.12 MPa, 6.9 ± 3.56 MPa and 12.7 ± 3.38 MPa. In the control group (Fig. 5a and b), there was no remnant of resin cement remaining on the fractured surface. Group R (Fig. 5c and d), which had the lowest shear bond strength (6.9 ± 3.56 MPa), showed adhesive failure at the zirconia/cement interface. Group Q (Fig. 5e and f), which had the highest shear bond strength (12.7 ± 3.38 MPa), exhibited adhesive failure with more remnants of the resin cement on zirconia surface.

4. Discussion

As revealed by 4-way ANOVA, the null hypothesis that there is no difference in the flexural strength and characteristics by modifying alumina airborne-particle abrasion protocols on monolithic zirconia could be rejected. In addition, the shear

Table 3
Mean and standard deviation in parenthesis of shear bond strength (MPa) of resin cement investigated before and after thermocycling.

Group	0 Thermocycles	5000 Thermocycles
A (Control)	6.7 (1.92)	3.0 (1.12)
B	11.3 (3.73)	6.9 (3.56)
C	11.6 (2.77)	8.3 (2.36)
D	12.8 (1.76)	8.5 (3.87)
E	13.3 (4.42)	8.4 (2.07)
F	11.8 (3.40)	8.6 (2.57)
G	11.7 (1.62)	8.8 (2.97)
H	14.8 (2.46)	9.4 (2.80)
I	12.7 (3.44)	8.9 (2.62)
J	13.7 (3.88)	12.1 (2.57)
K	12.2 (2.12)	11.3 (2.61)
L	14.7 (3.94)	10.3 (2.07)
M	15.3 (3.13)	11.4 (2.82)
N	15.5 (2.08)	10.4 (2.56)
O	15.3 (3.78)	11.1 (2.28)
P	18.1 (4.41)	12.6 (3.73)
Q	18.3 (3.64)	12.7 (3.38)
R	10.8 (2.52)	6.1 (2.84)
S	10.8 (3.16)	6.2 (1.36)
T	11.3 (0.56)	10.6 (3.51)
U	12.0 (1.99)	11.1 (3.71)
V	12.0 (3.70)	9.4 (2.82)
W	11.5 (0.61)	10.4 (2.89)
X	12.6 (3.69)	9.9 (2.39)
Y	12.1 (2.07)	9.8 (2.52)

bond strength of the alumina airborne-particle abraded monolithic zirconia surface after thermocycling was significantly higher than that of the 'as-received' specimen. These results support the rejection of the null hypothesis that shear bond strength of resin cement to the abraded monolithic zirconia surface would not be different from that to a 'as-received' one, and that thermocycling does not affect shear bond strength of resin cement to the abraded surface.

In this study, airborne-particle abrasion provided a powerful method for improvement of both flexural strength and bond strength of resin cement at the cost of a somewhat lower degree of reliability. According to Kosmac et al. [15], this finding is likely explained by considering two competing factors influencing the strength of surface-treated Y-TZP ceramics. One is residual surface compressive stresses which contribute to strengthening, and the other is the mechanically-induced surface flaws which cause strength degradation. Compressive stresses are formed due to $t \rightarrow m$ transformation, which increase the flexural strength of zirconia ceramics by resisting crack propagation [2,15,30,31]. However, under clinical conditions where the material is exposed to thermal and mechanical cycling in an aqueous environment over long periods, fracture initiation at lower levels of applied stress is enhanced [15]. The amount of tetragonal phase that is able to transform to monoclinic under compression is one of the main features of zirconia ceramics, because this determines the fracture toughness [44].

The variability in strength of ceramics is primarily due to the extreme sensitivity to the presence of cracks of different sizes [45]. For a given ceramic material, the distribution of crack size, shape, and orientation differs from sample to sample. Thus, Weibull proposed two parameter distribution functions to characterize the strength of brittle materials and the Weibull distribution function is widely used to model or characterize the flexural strength of various brittle materials including dental ceramics [41,42,45]. For Y-TZP, the flexural strength varies from 700 to 1200 MPa and the Weibull modulus from 10 to 18 [15,17,46,47]. In this study, the mean values of the monolithic zirconia characteristic strength ranged from 1212 to 2827 MPa, and Weibull modulus from 7 to 20. There were significant effects of airborne-particle size, notably the 25 and 50 μm particle sizes, on the flexural strength and Weibull characteristic strength, which generally also resulted in a decrease in reliability in all but two groups (Groups B and C). Interestingly, an increase in particle size (125 μm) produced a decrease in the flexural strength data and reliability (Table 2). Due to high stresses developed during abrasion with 125 μm particle size, severe surface cracks were formed which likely reduced the strength and reliability of the material [15,48]. The effect of the large-sized particles on the zirconia specimen may produce unstable flaws or substrate damage with microcracks.

Low particle velocity with small size, low pressure and low angle has a reduced rate of surface erosion [49], and hence it would appear that particles at 45° are more likely to safely abrade brittle substrates in combination with a low air stream pressure. At low velocity and relatively smaller particle sizes (25 and 50 μm), a significant increase in Weibull modulus and characteristic strength, representing an improvement in the reliability of the flexural strength data, was observed with a decrease in the incidence angle, whereas at high velocity and a 125 μm particle size, a decrease in the Weibull modulus and characteristic strength of the specimens was observed.

When an abrasive particle is pressed against the surface of the monolithic zirconia specimen, a contact stress field is generated which, for the various airborne-particle abrasion protocols used here, was able to reach a magnitude sufficient to induce the $t \rightarrow m$ transformation up to a depth of 10 μm, as shown in Fig. 3. In X-ray diffraction data, the amount of monoclinic phase (X_M) was increased with larger particle size, higher pressure, longer time and larger incidence angle. This is consistent with various *in vitro* studies which have shown that the amount of monoclinic phase produced varied according to these four factors [16,36]. Interestingly, in this study, the incidence angles factor took precedence over time factor in certain groups (Groups G and H, Groups K and L, Groups O and P, Groups S and T). Except the weakest conditions (Groups C and D) and the strongest conditions (Groups W and X), the same trends for variation in the incidence angle were shown over time under the same pressure conditions throughout the X-ray diffraction spectra. In addition, the combination of the incidence angle and the abrading time seemed more important than pressure in *m* transformation phase. All groups with protocols that included 2 bar, 20 s and 90° parameters exhibited higher X_M than those with protocols that called for 4 bar, 10 s and 45°.

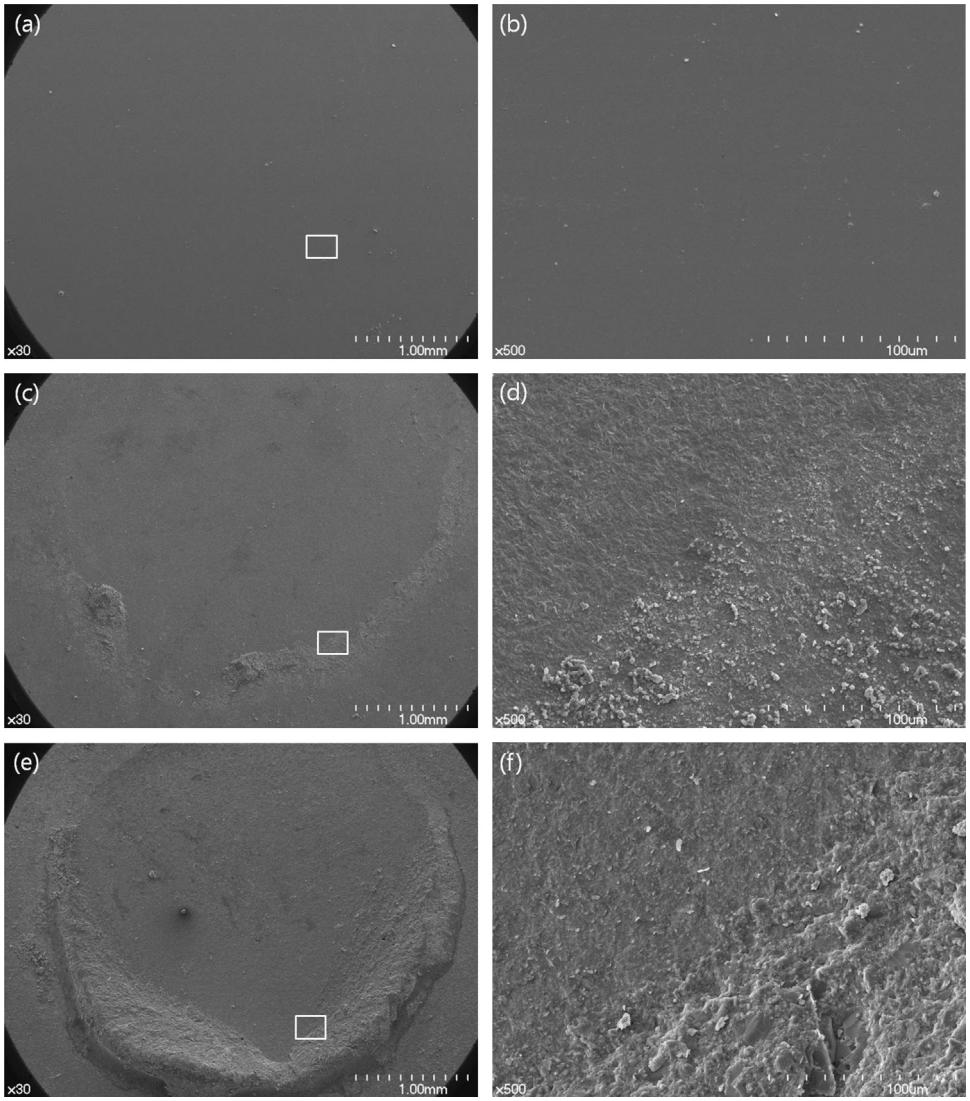

Fig. 5. Scanning electron micrographs (the left sides magnification × 30 and the right sides × 500) of zirconia surfaces: (a, b) Control group; (c, d) Group R which had the lowest shear bond strength to resin cement; (e, f) Group Q which had the highest shear bond strength to resin cement.

S_a data in our study suggest that the interaction of different size of particle, pressure, time and angle promote different topographic patterns on the monolithic zirconia ceramic surfaces. It is noteworthy that surface roughness of groups with 10 s and 90° was similar to that of groups with 20 s and 45° at the same pressure, and that the relative monoclinic phase contents were similar in both groups. It is possible that lower particle velocity may cause smaller surface fragments to be broken thereby increasing surface roughness without introducing more detrimental defects in spite of longer abrading time. With smaller particle sizes, it will then be favorable to either increase the incidence angle and shorten the abrading time or decrease the angle and extend the abrading time. When 125 μm-sized alumina was employed, the surface roughness (S_a) value increased reflecting the relative 'chipping' phenomenon at the zirconia surface.

Various *in vitro* studies have shown that airborne-particle abrasion with alumina is an essential step in achieving a durable bond to high strength ceramics [10,13,23,50]. However, despite the increase in bond strength between the resin cement and zirconia ceramics, the application of airborne-particle abrasion on such ceramics is controversial due to the possible introduction of flaws and microcracks [51,52]. As expected, the application of airborne-particle abrasion to monolithic zirconia specimens resulted in a significant increase in shear bond strength, as observed in the values of shear bond strength in both pre- and post-thermocycled specimens' compared to the 'as-received' monolithic zirconia specimens. In bonding with resin cement after thermocycling, the highest shear bond strength was observed in groups abraded with 50 μm particles, whereas the lowest shear bond strength in groups abraded with 125 μm. In other words, groups abraded with 125 μm exhibited significantly lower shear bond strength compared to the 50 μm abrasion-groups, despite having similar surface roughness levels. The difference in shear bond strength values of the two groups decreased after thermocycling. This finding suggested that thermocycling significantly reduces the shear bond strength

regardless of alumina particle size in airborne-particle abrasion. This result is in accordance with other studies showing the relative insignificance of the particle size difference in abrasion when the outcome of interest is the production of a durable bond between Y-TZP and resin cement [10,22,53]. Moreover, these results indicate that, while airborne-particle abrasion of monolithic zirconia produces superficial irregularities corresponding to the certain abrasion protocol, the effect of severe-sized undercuts is limited considering its contribution to the increase of surface roughness. Ultimately, the recommended mean size of alumina particle is 50 μm considering its ideal contribution to surface roughness and monoclinic phase, providing optimal shear bond strength, and its cleaning effect on the inner surface of restorations.

In this study, shear bond strengths were significantly decreased regardless of the size of alumina particle for surface treatment after 5000 thermocycles. Interaction of particle size × pressure × time was not significant before thermocycling; however, it became statistically significant after thermocycling. This change may suggest that the interaction of the three factors (particle size, pressure, time) maintains the long-term resin bond strength of monolithic zirconia ceramics [53].

5. Conclusion

In short, the interaction between the abrasive particle and the substrate surface clearly relies on complex interactions and cannot be explained by a simple theoretical model. The alteration of the flaw population of the specimen is often indiscriminate but may have dramatic effects on the longevity of a restoration. Airborne-particle abrasion with alumina increases the monolithic zirconia surface area and increases the surface area allowed, to an even greater extent, for the reaction between the resin cement and zirconia ceramics. This study suggests that airborne-particle abrasion with mean particle size of 50 μm, 4 bar and 20 s in both angles of incidence is effective for reliability of monolithic zirconia ceramics and for strong and durable bond formation with resin cement.

Acknowledgments

This study was supported by the research Grant no. 04-2012-0065 from the Seoul National University Dental Hospital Research Fund, Repubic of Korea. The monolithic Y-TZP ceramic materials (Zmatch Dentaim, Neobiotech, Seoul, Korea) used in this study were generously supplied by their manufacturers. We are indebted to Young-Ku Heo and Byoung-Soo Kim of Neobiotech for their supports and advices.

References

[1] B.E. Pjetursson, I. Sailer, M. Zwahlen, C.H. Hammerle, A systematic review of the survival and complication rates of all-ceramic and metal–ceramic reconstructions after an observation period of at least 3 years. Part I: single crowns, Clin. Oral Implant. Res. 18 (Suppl. 3) (2007) S73–S85.

[2] R.G. Luthardt, M. Holzhuter, O. Sandkuhl, V. Herold, J.D. Schnapp, E. Kuhlisch, M. Walter, Reliability and properties of ground Y-TZP-zirconia ceramics, J. Dent. Res. 81 (2002) 487–491.

[3] C.P. Ernst, P. Doz, U. Cohnen, E. Stender, B. Willershausen, In vitro retentive strength of zirconium oxide ceramic crowns using different luting agents, J. Prosthet. Dent. 93 (2005) 551–558.

[4] C. Larsson, P. Vult von Steyern, Five-year follow-up of implant-supported Y-TZP and ZTA fixed dental prostheses. A randomized, prospective clinical trial comparing two different material systems, Int. J. Prosthodont. 23 (2010) 555–561.

[5] J. Tinschert, K.A. Schulze, G. Natt, P. Latzke, N. Heussen, H. Spiekermann, Clinical behavior of zirconia-based fixed partial dentures made of DC-Zirkon: 3-year results, Int. J. Prosthodont. 21 (2008) 217–222.

[6] P. Triwatana, N. Nagaviroj, C. Tulapornchai, Clinical performance and failures of zirconia-based fixed partial dentures: a review literature, J. Adv. Prosthodont. 4 (2012) 76–83.

[7] F. Rojas-Vizcaya, Full zirconia fixed detachable implant-retained restorations manufactured from monolithic zirconia: clinical report after two years in service, J. Prosthodont. 20 (2011) 570–576.

[8] V. Preis, M. Behr, S. Hahnel, G. Handel, M. Rosentritt, In vitro failure and fracture resistance of veneered and full-contour zirconia restorations, J. Dent. 40 (2012) 921–928.

[9] F. Beuer, M. Stimmelmayr, J.F. Gueth, D. Edelhoff, M. Naumann, In vitro performance of full-contour zirconia single crowns, Dent. Mater. 28 (2012) 449–456.

[10] M. Kern, S.M. Wegner, Bonding to zirconia ceramic: adhesion methods and their durability, Dent. Mater. 14 (1998) 64–71.

[11] M.B. Blatz, A. Sadan, M. Kern, Resin–ceramic bonding: a review of the literature, J. Prosthet. Dent. 89 (2003) 268–274.

[12] M. Hummel, M. Kern, Durability of the resin bond strength to the alumina ceramic Procera, Dent. Mater. 20 (2004) 498–508.

[13] M.B. Blatz, A. Sadan, J. Martin, B. Lang, In vitro evaluation of shear bond strengths of resin to densely-sintered high-purity zirconium-oxide ceramic after long-term storage and thermal cycling, J. Prosthet. Dent. 91 (2004) 356–362.

[14] H. Lüthy, O. Loeffel, C.H.F. Hammerle, Effect of thermocycling on bond strength of luting cements to zirconia ceramic, Dent. Mater. 22 (2006) 195–200.

[15] T. Kosmac, C. Oblak, P. Jevnikar, N. Funduk, L. Marion, The effect of surface grinding and sandblasting on flexural strength and reliability of Y-TZP zirconia ceramic, Dent. Mater. 15 (1999) 426–433.

[16] H. Sato, K. Yamada, G. Pezzotti, M. Nawa, S. Ban, Mechanical properties of dental zirconia ceramics changed with sandblasting and heat treatment, Dent. Mater. J. 27 (2008) 408–414.

[17] A.R. Curtis, A.J. Wright, G.J. Fleming, The influence of surface modification techniques on the performance of a Y-TZP dental ceramic, J. Dent. 34 (2006) 195–206.

[18] D.P. Senyilmaz, W.M. Palin, A.C. Shortall, F.J. Burke, The effect of surface preparation and luting agent on bond strength to a zirconium-based ceramic, Oper. Dent. 32 (2007) 623–630.

[19] W.S. Oh, C. Shen, Effect of surface topography on the bond strength of a composite to three different types of ceramic, J. Prosthet. Dent. 90 (2003) 241–246.

[20] L.F. Valandro, M. Ozcan, M.C. Bottino, M.A. Bottino, R. Scotti, A.D. Bona, Bond strength of a resin cement to high-alumina and zirconia-reinforced ceramics: the effect of surface conditioning, J. Adhes. Dent. 8 (2006) 175–181.

[21] P. Derand, T. Derand, Bond strength of luting cements to zirconium oxide ceramics, Int. J. Prosthodont. 13 (2000) 131–135.

[22] Y. Tsuo, K. Yoshida, M. Atsuta, Effects of alumina-blasting and adhesive primers on bonding between resin luting agent and zirconia ceramics, Dent. Mater. J. 25 (2006) 669–674.

[23] Y. Zhang, B.R. Lawn, E.D. Rekow, V.P. Thompson, Effect of sandblasting on the long-term performance of dental ceramics, J. Biomed. Mater. Res. Part B: Appl. Biomater. 71 (2004) 381–386.

[24] Y. Zhang, B.R. Lawn, K.A. Malament, P. Van Thompson, E.D. Rekow, Damage accumulation and fatigue life of particle-abraded ceramics, Int. J. Prosthodont. 19 (2006) 442–448.
[25] T.K. Gupta, Strengthening by surface damage in metastable tetragonal zirconia, J. Am. Ceram. Soc. 63 (1980) 117.
[26] R. Mosharraf, M. Rismanchian, O. Savabi, A.H. Ashtiani, Influence of surface modification techniques on shear bond strength between different zirconia cores and veneering ceramics, J. Adv. Prosthodont 3 (2011) 221–228.
[27] A. Casucci, E. Osorio, R. Osorio, F. Monticelli, M. Toledano, C. Mazzitelli, M. Ferrari, Influence of different surface treatments on surface zirconia frameworks, J. Dent. 37 (2009) 891–897.
[28] P. Christel, A. Meunier, M. Heller, J.P. Torre, C.N. Peille, Mechanical properties and short-term in-vivo evaluation of yttrium-oxide-partially-stabilized zirconia, J. Biomed. Mater. Res. 23 (1989) 45–61.
[29] T. Sato, M. Shimada, Transformation of yttria-doped tetragonal ZrO_2 polycrystals by annealing in water, J. Am. Ceram. Soc. 68 (1985) 356–359.
[30] T. Kosmac, C. Oblak, P. Jevnikar, N. Funduk, L. Marion, Strength and reliability of surface treated Y-TZP dental ceramics, J. Biomed. Mater. Res. 53 (2000) 304–313.
[31] M. Guazzato, L. Quach, M. Albakry, M.V. Swain, Influence of surface and heat treatments on the flexural strength of Y-TZP dental ceramic, J. Dent. 33 (2005) 9–18.
[32] A. Della Bona, T.A. Donassollo, F.F. Demarco, A.A. Barrett, J.J. Mecholsky Jr., Characterization and surface treatment effects on topography of a glass-infiltrated alumina/zirconia-reinforced ceramic, Dent. Mater. 23 (2007) 769–775.
[33] R.C. Oyague, F. Monticelli, M. Toledano, E. Osorio, M. Ferrari, R. Osorio, Effect of water aging on microtensile bond strength of dual-cured resin cements to pre-treated sintered zirconium-oxide ceramics, Dent. Mater. 25 (2009) 392–399.
[34] R.C. de Oyague, F. Monticelli, M. Toledano, E. Osorio, M. Ferrari, R. Osorio, Influence of surface treatments and resin cement selection on bonding to densely-sintered zirconium-oxide ceramic, Dent. Mater. 25 (2009) 172–179.
[35] M. Uo, G. Sjogren, A. Sundh, M. Goto, F. Watari, M. Bergman, Effect of surface condition of dental zirconia ceramic (Denzir) on bonding, Dent. Mater. J. 25 (2006) 626–631.
[36] L. Hallmann, P. Ulmer, E. Reusser, C.H. Hammerle, Surface characterization of dental Y-TZP ceramic after air abrasion treatment, J. Dent. 40 (2012) 723–735.
[37] M. Özcan, J. Raadschelders, P. Vallittu, L. Lassilla, Effect of particle deposition parameters on silica coating of zirconia using a chairside air-abrasion device, J. Adhes. Dent. 15 (2013) 211–214.
[38] M. Özcan, R.M. Melo, R.O.A. Souza, J.P.B. Machado, L. Felipe Valandro, M.A. Botttino, Effect of air-particle abrasion protocols on the biaxial flexural strength, surface characteristics and phase transformation of zirconia after cyclic loading, J. Mech. Behav. Biomed. Mater. 20 (2013) 19–28.
[39] R.O.A. Souza, L.F. Valandro, R.M. Melo, J.P.B. Machado, M.A. Bottino, M. Özcan, Air–particle abrasion on zirconia ceramic using different protocols: effects on biaxial flexural strength after cyclic loading, phase transformation and surface topography, J. Mech. Behav. Biomed. Mater. 26 (2013) 155–163.
[40] R.C. Garvie, Phase analysis in zirconia systems, J. Am. Ceram. Soc. 55 (1972) 303–305.
[41] W. Weibull, A statistical distribution function of wide applicability, J. Appl. Mech. 18 (1951) 293–297.
[42] J.E. Ritter, Predicting lifetimes of materials and material structures, Dent. Mater. 11 (1995) 142–146.
[43] J.B. Quinn, G.D. Quinn, A practical and systematic review of Weibull statistics for reporting strengths of dental materials, Dent. Mater. 26 (2010) 135–147.
[44] A. Juy, M. Anglada, Surface phase transformation during grinding of Y-TZP, J. Am. Ceram. Soc. 90 (2007) 2618–2621.
[45] B. Basu, D. Tiwari, D. Kundu, R. Prasad, Is Weibull distribution the most appropriate statistical strength distribution for brittle materials?, Ceram. Int. 35 (2009) 237–246.
[46] J. Tinschert, G. Natt, N. Mohrbotter, H. Spiekermann, K.A. Schulze, Lifetime of alumina- and zirconia ceramics used for crown and bridge restorations, J. Biomed. Mater. Res. Part B: Appl. Biomater. 80B (2007) 317–321.
[47] R.G. Luthardt, M.S. Holzhüter, H. Rudolph, V. Herold, M.H. Walter, CAD/CAM-machining effects on Y-TZP zirconia, Dent. Mater. 20 (2004) 655–662.
[48] H. Wang, M.N. Aboushelib, A.J. Feilzer, Strength influencing variables on CAD/CAM zirconia frameworks, Dent. Mater. 24 (2008) 633–638.
[49] O. Addison, P.M. Marquis, G.J. Fleming, The impact of modifying alumina air abrasion parameters on the fracture strength of a porcelain laminate restorative material, Dent. Mater. 23 (2007) 1332–1341.
[50] S.M. Wegner, M. Kern, Long-term resin bond strength to zirconia ceramic, J. Adhes. Dent. 2 (2000) 139–147.
[51] S.M. Wegner, W. Gerdes, M. Kern, Effect of different artificial aging conditions on ceramic-composite bond strength, Int. J. Prosthodont. 15 (2002) 267–272.
[52] S.S. Atsu, M.A. Kilicarslan, H.C. Kucukesmen, P.S. Aka, Effect of zirconium-oxide ceramic surface treatments on the bond strength to adhesive resin, J. Prosthet. Dent. 95 (2006) 430–436.
[53] J.H. Phark, S. Duarte Jr., M. Blatz, A. Sadan, An in vitro evaluation of the long-term resin bond to a new densely sintered high-purity zirconium-oxide ceramic surface, J. Prosthet. Dent. 101 (2009) 29–38.